Phonon Spectra, Nearest Neighbors, and Mechanical Stability of Disordered Colloidal Clusters with Attractive Interactions

Peter J. Yunker,[1] Ke Chen,[1] Zexin Zhang,[2,3] and A. G. Yodh[1]

[1]*Department of Physics and Astronomy, University of Pennsylvania, Philadelphia, Pennsylvania 19104, USA*
[2]*Center for Soft Condensed Matter Physics and Interdisciplinary Research, Soochow University, Suzhou 215006, China*
[3]*Complex Assemblies of Soft Matter, CNRS-Rhodia-UPenn UMI 3254, USA*

(Received 1 March 2011; published 1 June 2011)

We investigate the influence of morphology and size on the vibrational properties of disordered clusters of colloidal particles with attractive interactions. Spectral features of the vibrational modes are found to depend strongly on the average number of nearest neighbors, $\overline{NN}$, but only weakly on the number of particles in each glassy cluster. In particular, the median phonon frequency, ω_{med}, is constant for $\overline{NN} < 2$ and then grows linearly with $\overline{NN}$ for $\overline{NN} > 2$. This behavior parallels concurrent observations about local isostatic structures, which are absent in clusters with $\overline{NN} < 2$ and then grow linearly in number for $\overline{NN} > 2$. Thus, cluster vibrational properties appear to be strongly connected to cluster mechanical stability, and the scaling of ω_{med} with $\overline{NN}$ is reminiscent of the jamming transition. Simulations of random networks of springs corroborate observations.

DOI: 10.1103/PhysRevLett.106.225503 PACS numbers: 63.50.Lm, 61.43.Fs, 63.22.Kn, 64.70.kj

The phase behavior and vibrational properties of ensembles of repulsive particles are determined largely by the packing fraction [1]. Samples of monodisperse spheres, for example, gain structural order and eventually crystallize with increasing packing fraction [1], giving rise to low frequency plane-wave-like phonon modes. In a related vein, ensembles of polydisperse spheres gain contacts with increased packing fraction, leading to vitrification [2] and ''soft phonon modes'' whose properties depend on the average number of interparticle contacts [3]. In contrast to these ''space-filling'' systems, particles with strong attractive interactions can form solidlike phases at low macroscopic packing fractions [4]. Dilute gels, for example, mechanically percolate across large distances [5], and disordered clusters containing relatively few particles often self-assemble into structures with a large local packing fraction [6]. In this Letter we explore how cluster morphology and cluster size affect the vibrational properties of disordered materials held together by strong attractive interactions. The new understanding thus gained holds the potential to elucidate the fundamental differences between glassy materials composed of particles with attractive versus repulsive interactions, to uncover connections of cluster vibrational spectra with cluster mechanical stability and the jamming problem, and to discover attributes of a disordered cluster that endow it with the properties of bulk glasses.

To date, a diverse collection of disordered systems has been observed to display surprising commonality in the systems' vibrational properties. Such systems include molecular [7], polymer [8], and colloidal glasses [9]. These disordered solids exhibit an excess of low frequency modes that are believed important for their mechanical and thermal properties [10]. The low frequency modes also appear connected to scaling and mechanical behaviors of repulsive spheres near the zero-temperature jamming transition. At the jamming point, such disordered packings are ''isostatic''; i.e., they have exactly the number of contacts per particle required for mechanical stability. If a single contact is removed, the packing is no longer stable. Interestingly, marginal stability permits particle displacements that maintain isostaticity without energy cost; these motions are manifest as low frequency ''soft'' phonon modes [3,11]. When the sample packing fraction is increased above the jamming transition, the number of contacts per particle increases, the system is stabilized [12], and the number of soft modes is found to decrease [3]. In fact, the minimum soft mode frequency is predicted to increase linearly with the number of contacts per particle above the isostatic requirement [3]. Recent experiments have found some of these trends in thermal packings of repulsive particles [9], but application of such concepts to systems with attractive interactions has proven difficult. Ensembles of attractive particles can achieve isostaticity at an arbitrary packing fraction, and even when they do not have enough contacts to be isostatic as a whole, the attractive systems can still have local mechanically stable regions [11,13]. Therefore, the study of vibrational properties in clusters of attractive particles can provide useful clues about underlying mechanisms responsible for the mechanical properties of disordered solids.

Herein we experimentally investigate the influence of cluster morphology and size on the vibrational properties of disordered clusters of colloidal particles with attractive interactions. The disordered clusters with high local packing fractions are formed in water-lutidine suspensions where wetting effects induce fluid-mediated attractions between micron-sized polystyrene particles. Each cluster

is characterized by the number of particles it contains (N), an average number of nearest neighbors ($\overline{NN}$), and a number of local isostatic configurations (N_{Iso}). Displacement correlation matrix techniques employed in recent papers [9] are used to determine the phonon density of states of corresponding ''shadow'' attractive glass clusters with the same geometric configuration and interactions as the ''source'' experimental colloidal system but absent damping.

Surprisingly, the spectra and character of vibrational modes depend strongly on $\overline{NN}$ but only weakly on N. The median phonon frequency, ω_{med}, which characterizes the distribution of low and high frequency modes, is observed to be essentially constant for $\overline{NN} < 2$, and then grows linearly with $\overline{NN}$ for $\overline{NN} > 2$. This behavior parallels concurrent observations about local isostatic structures, which are absent in clusters with $\overline{NN} < 2$ and then grow linearly in number for $\overline{NN} > 2$. Thus cluster vibrational properties appear to be strongly connected to cluster mechanical microstructure and stability (i.e., the fraction of locally isostatic regions), and the scaling of ω_{med} with $\overline{NN}$ is reminiscent of the behavior of packings of spheres with repulsive interactions at the jamming transition, even though these clusters are not jammed in the macroscopic sense (e.g., by the criteria used in [12,13]). Simulations of random networks of springs corroborate observations and further suggest that connections between phonon spectra and nearest neighbor number are generic to disordered networks.

The experiments employ bidisperse suspensions of micron-sized polystyrene particles (Invitrogen), with diameters $d_S = 1.5$ m and $d_L = 1.9$ m, and number ratio 1:2, respectively. Particles were suspended in a mixture of water and 2, 6-lutidine near its critical composition, i.e., with a lutidine mass fraction of 0.28. Colloidal particles suspended in this near-critical binary mixture experience temperature-dependent repulsive or attractive interactions, whose origins can be fluid-mediated wetting, as in the current experiments, or critical Casimir forces [14]. Interparticle potentials are shown in Fig. 1(a) [15]. Particles are confined between two glass coverslips (Fisher) with a spacing of $\sim(1.1 \quad 0.05)d_L$, making the sample system quasi-two-dimensional. The glass cell was treated with NaOH, so the particle-wall interaction potential is repulsive at relevant temperatures [16]. Many different disordered particle clusters of various sizes and shapes are created by first suspending particles deep in the repulsive regime (300.15 K), and then increasing the sample temperature (to 306.5 K) *in situ*. Some clusters self-assemble while other clusters are assembled with the aid of laser tweezers [15,17]. Samples were equilibrated for about six hours, and video data were collected at 10 frames per second [15].

As noted above, the particle cluster structure is characterized by several factors, including average number of

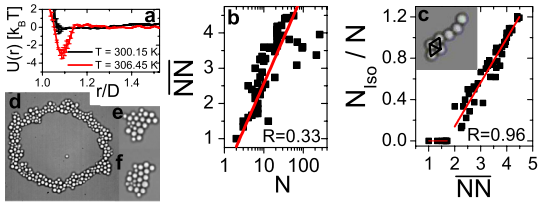

FIG. 1 (color online). (a) Plot of the temperature-dependent ($T = 300.15$ K and 306.45 K) interparticle potential, $u(r)$, as a function of particle separation (r) normalized by particle diameter (D). The temperature dependence is induced by wetting effects in near-critical water-lutidine mixtures. (b) Plot summarizing N and $\overline{NN}$ in every cluster. (c) The number fraction of locally isostatic configurations per particle, N_{Iso}/N is plotted versus the average number of nearest neighbors, $\overline{NN}$. Solid lines are linear fits within two separate regimes. Inset: Experimental snapshot of an $N = 7$ cluster with two locally isostatic triangles. Black lines indicate the triangles. (d–f) Experimental snapshots of clusters with $N = 261$, $\overline{NN} = 3.95$ (d), $N = 22$, $\overline{NN} = 3.91$ (e), and $N = 22$, $\overline{NN} = 4.09$ (f).

nearest neighbors per particle and number of locally isostatic configurations. Neighbors are defined as particles spatially separated by less than a cutoff distance equal to the first minimum in the particle pair correlation function. Local isostatic regions consist of three particles (a, b, and c) that are mutually nearest neighbors (i.e., a and b are neighbors, a and c are neighbors, b and c are neighbors). Plots summarizing N, $\overline{NN}$, and N_{Iso} for each cluster studied are shown in Figs. 1(b) and 1(c), along with experimental snapshots of selected clusters [Figs. 1(d)–1(f)]. Note that $\overline{NN}$ tends to increase with increasing N for our distribution of cluster sizes, but that the increase is not monotonic. The dependence of N_{Iso} on $\overline{NN}$ exhibits two regimes. Specifically, N_{Iso}/N is 0 for $\overline{NN} < 2$, becomes nonzero abruptly at $\overline{NN} = 2$, and then grows linearly with $\overline{NN}$ for $\overline{NN} > 2$. Thus, we identify $\overline{NN} = 2$ as the ''local isostatic'' point.

The measured displacement covariance matrix [9] was employed to extract vibrational modes of the shadow colloidal clusters, which share the same geometric configuration and interactions of the experimental colloidal system, but are undamped. Comparing the frequency spectra of clusters with small N can be challenging, since not enough modes are present for clear identification of a traditional ''peak'' frequency, and since fluctuations can significantly shift mode frequency. For these reasons we choose to characterize each cluster's density of states by its median frequency, ω_{med}. Plots of ω_{med} as a function of the average number of nearest neighbors, $\overline{NN}$, and as a function of the total number of cluster particles, N (at nearly fixed $\overline{NN}$), are shown in Figs. 2(a) and 2(b).

Surprisingly, ω_{med} has little correlation with N, exhibiting linear correlation coefficients of $R = 0.29$. This effect is even more apparent when the number of nearest neighbors is held nearly constant [Fig. 2(b)]. However, ω_{med}

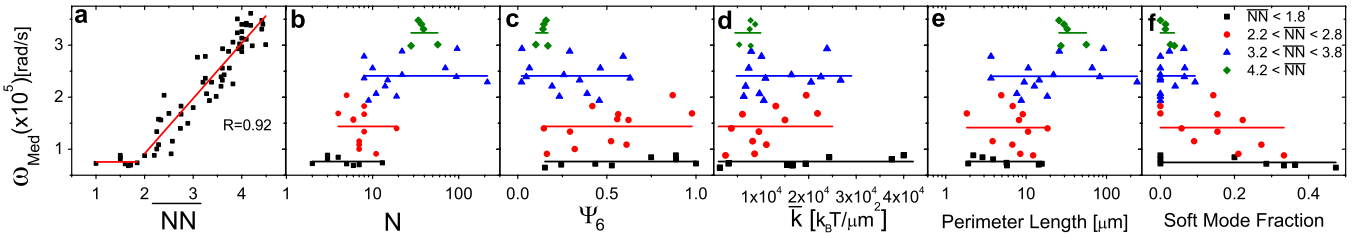

FIG. 2 (color online). (a) Median frequency, ω_{med}, versus average number of nearest neighbors, $\overline{NN}$. Two regimes exist. For $\overline{NN} < 2$, ω_{med} is constant (line is constant fit). For $\overline{NN} > 2$, ω_{med} increases linearly with $\overline{NN}$ (line is a linear fit). In (b–d), $\overline{NN}$ in different sample types is indicated by plotting $\overline{NN} < 1.8$ as black squares, $2.2 < \overline{NN} < 2.8$ as red circles, $3.2 < \overline{NN} < 3.8$ as blue triangles, $4.2 < \overline{NN}$ as green diamonds. Lines are best constant fits. (b) ω_{med} versus number of particles, N. (c) ω_{med} versus orientational order parameter, ψ_6. (d) ω_{med} versus average total nearest neighbor spring constant, k. (e) ω_{med} versus perimeter length, i.e., the contour length of the cluster exterior. (f) ω_{med} plotted versus the fraction of soft modes, i.e., the fraction of modes that cost little to no energy.

depends strongly on the average number of nearest neighbors ($\overline{NN}$). We observe two distinct regimes. For $\overline{NN} < 2$, ω_{med} is constant. For $\overline{NN} > 2$, ω_{med} increases linearly with $\overline{NN}$ ($R = 0.92$). Interestingly, the dependence of ω_{med} on $\overline{NN}$ is very similar to the dependence of the number fraction of locally isostatic configurations per particle, i.e., N_{Iso}/N, on $\overline{NN}$ [Fig. 1(b)]. These observations suggest that the vibrational properties of disordered clusters are strongly dependent on the presence of locally rigid elements. Note that creating a rigid triangle in a locally unstable region may remove a zero-frequency soft mode, but creating a locally rigid triangle in a stable region will not. Thus the observed correspondence between ω_{med} and N_{Iso}/N is surprising, especially for larger values of NN where locally soft regions are unlikely to appear, i.e., $NN > 3.0$ [11]. Furthermore, we expect to observe a correlation between ω_{med} and N for our cluster distribution, because $\overline{NN}$ tends to increase with N for typical cluster distributions. Thus, while we would expect the vibrational spectra of a disordered attractive cluster to become similar to the vibrational spectra of a bulk glass as the total number of particles in the cluster increases, the underlying mechanism for this effect originates from the average number of nearest neighbors in the cluster, rather than the total particle number in the cluster.

Interestingly, the dependence of ω_{med} on $\overline{NN}$ is also reminiscent of the behavior of hard spheres in the vicinity of the zero-temperature jamming transition [4]. In the jamming case, the characteristic frequency, ω , of excess quasilocalized or soft modes increases linearly with $\overline{NN}$ when $\overline{NN} > \overline{NN}_C$, where $\overline{NN}_C$ is the number of contacts necessary for isostaticity. Similarly, in our experiments with attractive particles, ω_{med} increases linearly with $\overline{NN}$ when $\overline{NN} > 2$ and when locally rigid elements are present, despite the fact that these clusters are not jammed in the traditional sense [12,13]. In thermal experiments with repulsive particles, ω_{med} shows a strong linear correlation with ω ($R = 0.96$), and ω_{med} has a strong linear relationship with $\overline{NN}$ [9]. Thus our observations suggest that similar "jamming transition" physics may control properties of both highly packed glasses and disordered clusters composed of particles with attractive interactions at a low (overall) packing fraction.

As a final demonstration of the importance of $\overline{NN}$ versus N, consider two clusters that look very different [Figs. 1(d) and 1(e)], but that have almost the same $\overline{NN}$. These clusters have similar characteristic frequencies [i.e., $\omega_{\mathrm{med}} = 3.0\ \ 10^5(0.05)$[rad/s and $3.1\ \ 10^5(0.05)$[rad/s for Figs. 1(d) and 1(e), respectively]. On the other hand, two clusters that contain the exact same number of particles, but have different $\overline{NN}$ (Figs. 1(e) and 1(f)), possess a set of very different characteristic frequencies [$\omega_{\mathrm{med}} = 3.1\ \ 10^5(0.05)$[rad/s and $3.6\ \ 10^5(0.05)$[rad/s for Figs. 1(e) and 1(f), respectively].

As per other calculable cluster properties, ω_{med} does not appear to correlate strongly with many traditional structural quantities, including the bond orientational order parameter, ψ_6 [18], the average stiffness between nearest neighbor pairs, k [19], and the cluster perimeter length, i.e., the contour length of the cluster exterior. These parameters do not correlate strongly with ω_{med}, when $\overline{NN}$ is held approximately constant [Figs. 2(c)–2(e)]. Thus, simple ideas for the effects based on surface area or perimeter length are not sufficient to explain experimental observations. Additionally, the fraction of soft modes does not correlate strongly with ω_{med}, when $\overline{NN}$ is held approximately constant [Fig. 2(f)] [15].

As a final check on the importance of structural quantities other than $\overline{NN}$, we explored the calculated spectra of randomly generated networks of springs. Random networks of springs, expressed as matrices, K_{ij}, were generated following simple rules that ensure the matrices contain information about N and $\overline{NN}$ [20]: (1) each element, ij, in the matrix represents the spring constant between particle or coordinate i and particle or coordinate j; (2) the number of rows or columns in these symmetric matrices is twice the number of particles, representing each coordinate of each particle; (3) the number of off-diagonal elements greater than zero is equivalent to the number of nearest neighbors; (4) diagonal elements are set such that

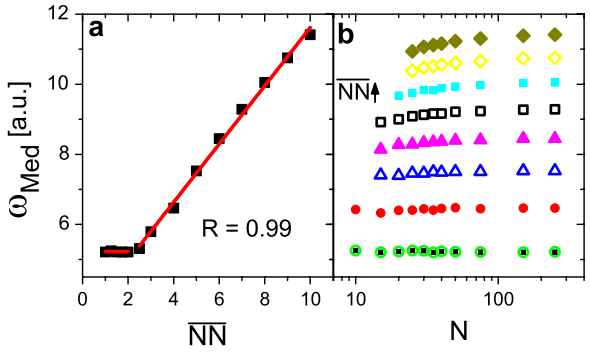

FIG. 3 (color online). (a) Median frequency, ω_{med}, plotted versus average number of nearest neighbors, $\overline{NN}$, from simulations of random matrices. (b) Median frequency, ω_{med}, plotted versus number of particles, N, from random matrices with $\overline{NN} = 1$ (solid black squares), 2 (open circles), 3 (solid circles), 4 (open triangles), 5 (solid triangles), 6 (open squares), 7 [solid gray (blue) squares], 8 (open diamonds), and 9 (solid diamonds).

the sum of each row or column is zero, ensuring translational invariance. Thus N and $\overline{NN}$ can be varied independently. For every combination of N and $\overline{NN}$, 10 000 random matrices are generated. ω_{med} is calculated from the combination of all generated frequencies (Fig. 3). Note that many of these networks cannot be duplicated in real experimental systems, since nearest neighbor pairings are assigned at random and not based on proximity. Nevertheless, we found that ω_{med} follows the same trends in these simulations as observed in our experiments: ω_{med} has little or no correlation with N (i.e., with $\overline{NN}$ held constant, ω_{med} changes by less than 5%), but exhibits a strong correlation with $\overline{NN}$ ($R > 0.99$). Thus ω_{med} appears to be the result of network connectivity, rather than specific structure.

In conclusion, the spectra and character of vibrational modes in disordered ''attractive'' clusters depend strongly on the average number of nearest neighbors and the number of locally isostatic configurations, but do not depend strongly on the number of particles in the cluster. The fact that ω_{med} depends on $\overline{NN}$, but not on the total number and packing fraction, is reminiscent of network glasses (e.g., silica [21]). Network glasses are composed of particles (e.g., molecules) that have directional bond forming interactions which set $\overline{NN}$ [22], leading to the formation of solids at low packing fractions. In fact, the vibrational [23] and mechanical [24] properties of network glasses are believed to depend strongly on $\overline{NN}$. Thus, the disordered clusters we have introduced could serve as a convenient model system for network glasses and their many applications (e.g., noncrystalline semiconductors [25]).

We thank Piotr Habdas, Carl Goodrich, Andrea Liu, and Tim Still for helpful discussions. We gratefully acknowledge financial support from the National Science Foundation through the PENN MRSEC DMR-0520020, DMR-0804881, and NASA NNX08AO0G.

[1] W. G. Hoover and F. H. Ree, J. Chem. Phys. **49**, 3609 (1968); P. N. Pusey and W. van Megen, Nature (London) **320**, 340 (1986).
[2] A. van Blaaderen and P. Wiltzius, Science **270**, 1177 (1995).
[3] M. Wyart, S. R. Nagel, and T. A. Witten, Europhys. Lett. **72**, 486 (2005).
[4] E. Zaccarelli, J. Phys. Condens. Matter **19**, 323 101 (2007).
[5] M. Y. Lin *et al.*, Nature (London) **339**, 360 (1989).
[6] G. Meng *et al.*, Science **327**, 560 (2010); P. J. Lu *et al.*, Phys. Rev. Lett. **96**, 028306 (2006).
[7] A. P. Sokolov *et al.*, Phys. Rev. Lett. **69**, 1540 (1992).
[8] B. Frick and D. Richter, Science **267**, 1939 (1995).
[9] D. Kaya *et al.*, Science **329**, 656 (2010); A. Ghosh *et al.*, Phys. Rev. Lett. **104**, 248305 (2010); K. Chen *et al.*, Phys. Rev. Lett. **105**, 025501 (2010).
[10] R. O. Pohl, X. Liu, and E. Thompson, Rev. Mod. Phys. **74**, 991 (2002).
[11] D. J. Jacobs and M. F. Thorpe, Phys. Rev. Lett. **75**, 4051 (1995).
[12] C. S. O'Hern *et al.*, Phys. Rev. Lett. **88**, 075507 (2002).
[13] G. Lois, J. Blawzdziewicz, and C. S. O'Hern, Phys. Rev. Lett. **100**, 028001 (2008).
[14] D. Beysens and T. Narayanan, J. Stat. Phys. **95**, 997 (1999); C. Hertlein *et al.*, Nature (London) **451**, 172 (2008).
[15] See supplemental material at http://link.aps.org/supplemental/10.1103/PhysRevLett.106.225503 for more information on the experimental system and analysis.
[16] F. Soyka *et al.*, Phys. Rev. Lett. **101**, 208301 (2008).
[17] D. G. Grier, Nature (London) **424**, 810 (2003).
[18] $\psi_6 = 1/N\sum_{j=1...N}\sum_{k=1...NN_j}\exp(i\theta_{jk}\pi/3)NN_j$, where $_{jk}$ is the angle between particles j and k, and NN_j is the number of neighbors for particle j.
[19] $k = 1/N\sum_{i=1...N}\sum_{j=1...NN_i}|K_{ij}|/NN_i$.
[20] M. Wyart, Europhys. Lett. **89**, 64 001 (2010); V. Gurarie and J. T. Chalker, Phys. Rev. Lett. **89**, 136801 (2002); Y. M. Beltukov and D. A. Parshin, arXiv:org/abs/1011.2955.
[21] P. H. Gaskell and D. J. Wallis, Phys. Rev. Lett. **76**, 66 (1996).
[22] F. Sciortino, Eur. Phys. J. B **64**, 505 (2008).
[23] W. A. Kamitakahara *et al.*, Phys. Rev. B **44**, 94 (1991).
[24] M. Zhang *et al.*, J. Non-Cryst. Solids **151**, 149 (1992).
[25] T. Kamiya, K. Nomura, and H. Hosono, Sci. Tech. Adv. Mater. **11**, 044 305 (2010).